Received: 2 September 2022 | Revised: 2 November 2022 | Accepted: 8 November 2022

DOI: 10.1111/mec.16787

ORIGINAL ARTICLE

MOLECULAR ECOLOGY WILEY

# Initiation of speciation across multiple dimensions in a rock-restricted, tropical lizard

Stephen M. Zozaya[1] | Luisa C. Teasdale[1,2] | Leonardo G. Tedeschi[1] | Megan Higgie[3] | Conrad J. Hoskin[3] | Craig Moritz[1]

[1]Research School of Biology, Australian National University, Australian Capital Territory, Canberra, Australia

[2]Department of Molecular Biology, Max Planck Institute for Developmental Biology, Tübingen, Germany

[3]College of Science and Engineering, James Cook University, Queensland, Townsville, Australia

**Correspondence**
Stephen M. Zozaya, Research School of Biology, Australian National University, Canberra 2601, ACT, Australia.
Email: stephen.zozaya@anu.edu.au

**Funding information**
Australian Geographic Society; Australian Research Council, Grant/Award Number: DP210102267 and FL110100104

**Handling Editor:** Sean D Schoville

## Abstract

Population isolation and concomitant genetic divergence, resulting in strong phylogeographical structure, is a core aspect of speciation initiation. If and how speciation then proceeds and ultimately completes depends on multiple factors that mediate reproductive isolation, including divergence in genomes, ecology and mating traits. Here we explored these multiple dimensions in two young (Plio-Pleistocene) species complexes of gekkonid lizards (*Heteronotia*) from the Kimberley–Victoria River regions of tropical Australia. Using mitochondrial DNA screening and exon capture phylogenomics, we show that the rock-restricted *Heteronotia planiceps* exhibits exceptional fine-scale phylogeographical structure compared to the codistributed habitat generalist *Heteronotia binoei*. This indicates pervasive population isolation and persistence in the rock-specialist, and thus a high rate of speciation initiation across this geographically complex region, with levels of genomic divergence spanning the "grey zone" of speciation. Proximal lineages of *H. planiceps* were often separated by different rock substrates, suggesting a potential role for ecological isolation; however, phylogenetic incongruence and historical introgression were inferred between one such pair. Ecomorphological divergence among lineages within both *H. planiceps* and *H. binoei* was limited, except that limestone-restricted lineages of *H. planiceps* tended to be larger than rock-generalists. By contrast, among-lineage divergence in the chemical composition of epidermal pore secretions (putative mating trait) exceeded ecomorphology in both complexes, but with less trait overlap among lineages in *H. planiceps*. This system—particularly the rock-specialist *H. planiceps*—highlights the role of multidimensional divergence during incipient speciation, with divergence in genomes, ecomorphology and chemical signals all at play at very fine spatial scales.

**KEYWORDS**
chemical signals, ecomorphology, genomics, phylogeography, reptiles, speciation

## 1 | INTRODUCTION

Speciation is often a multidimensional process, with reproductive isolation resulting from various combinations of divergence in genomes, ecology and associated phenotypic traits, and mate preference (Coyne & Orr, 2004; Kirkpatrick & Ravigné, 2002; Sobel et al., 2010). In some taxa, geographical isolation and concomitant genomic divergence precedes phenotypic divergence, resulting in "cryptic species" complexes that can remain distinct even following secondary contact (e.g., Singhal & Moritz, 2013). This can occur when different mutations arise and are fixed among allopatric populations adapting to similar selection pressures, a process termed "mutation-order speciation" (Nosil & Flaxman 2011). In others, ecologically driven divergent selection can result in rapid phenotypic differentiation and speciation, which can happen with or without gene flow (Schluter, 2009). On top of all this, traits influencing mate choice (mating traits) can diverge through sexual selection (Ritchie, 2007) and local adaptation (e.g., Endler, 1992; Hoskin & Higgie, 2010), including through reproductive character displacement by reinforcement when populations in secondary contact are subject to strong genetic incompatibilities (Butlin, 1987; Howard, 1993). In many cases, however, nascent species can go extinct through demographic processes, competition or merging with other populations when reproductive isolation is incomplete—processes captured in models of protracted or ephemeral speciation (Etienne & Rosindell, 2012; Rosenblum et al., 2012).

In phenotypically conservative groups, analysis of phylogeographical structure often identifies major spatial discontinuities in genetic diversity, reflecting historical isolation among metapopulations. Such strong phylogeographical structure has long been regarded as an important dimension of speciation initiation (e.g., Avise et al., 1998). This can be especially prevalent in low-dispersal species with strong niche conservatism (Kozak & Wiens, 2006; Wiens, 2004), with the initiation of speciation being driven by environmentally heterogenous landscapes that fragment populations and isolate them to similar but geographically separated environments. This is in contrast to ecological speciation, where adaptation to *different* environments—niche divergence—initiates speciation. Strong phylogeographical structure also presents a challenge to statistical species delimitation, where populations diverging along the "speciation continuum" can be over-split using phylogenomic tree-based methods alone (Chan et al., 2022; Leaché et al., 2019; Sukumaran & Knowles, 2017), especially when geographical sampling is sparse (Chambers & Hillis, 2020). It follows that studies of the speciation process and recognition of species should examine multiple dimensions that potentially influence reproductive isolation, including genomic divergence, ecological separation, mating traits and other relevant phenotypic changes—the essence of integrative taxonomy (Padial et al., 2010). Additionally, sampling should be as dense as possible to fully capture variation within and among nascent species.

We apply this integrative approach to two species complexes of gekkonid lizards from the Kimberley and Victoria River regions of the Australian monsoonal tropics, an area in which most species of low-dispersal vertebrates have strong phylogeographical structure (e.g., Fenker et al., 2021; Laver et al., 2017, 2018; Moritz et al., 2018; Oliver et al., 2012, 2019; Potter et al., 2012). This region of northwestern Australia is geologically complex, dominated by Proterozoic sandstone plateaus in the north separated by lower relief basalt intrusions, rugged sandstone ranges to the south and outcroppings of Devonian limestone system bordering the vast Australian arid zone (Pepper & Keogh, 2014). Climatically, the area is dominated by the summer monsoon, with high temperatures and a pronounced rainfall gradient from the wet northwest to the arid south and east. Across this region, two species of *Heteronotia* geckos co-occur (Figure 1a): *Heteronotia binoei* (Gray, 1845), a terrestrial habitat generalist that is found across much of Australia; and *Heteronotia planiceps* Storr, 1989, a rock-associated species that is endemic to the Kimberley–Victoria River regions. Previous sampling and multilocus sequencing of *H. binoei* has identified multiple species-level phylogeographical lineages across tropical Australia, including in the Kimberley and Victoria River regions (Fujita et al., 2010; Moritz et al., 2016; Zozaya et al., 2022a). Preliminary multilocus sequencing has also revealed strong genetic differences among some *H. planiceps*, but geographical sampling was limited (Oliver et al., 2017; Pepper et al., 2011).

The radiation of *Heteronotia* as a whole is probably Pliocene or late Miocene in age with Plio-Pleistocene diversification within each of *H. binoei* and *H. planiceps* (Fujita et al., 2010; Oliver et al., 2017), thus offering an opportunity to investigate recent and ongoing divergence processes. Morphological variation within species of *Heteronotia* is modest—reflected by the group's long-unresolved taxonomy—although there is evidence of habitat-driven phenotypic divergence among some eastern lineages of *H. binoei* (Riedel et al., 2021). A recent study of northeastern Australian lineages of *H. binoei* demonstrated that chemical composition of male epidermal pore secretions (a putative lizard mating trait; Kabir et al., 2020; Martín & López, 2014) has diverged more among sympatric and parapatric lineages than has ecomorphology (Zozaya et al., 2019). These recent discoveries pave the way for investigating mate-recognition signals in diverging lineages alongside more commonly studied genetic and morphological characters.

Here, we combine dense spatial sampling with sequencing of mitochondrial DNA (mtDNA) and >500 nuclear exons to resolve phylogeographical structure in these two species complexes across the Kimberley–Victoria River region. Given the association of *H. planiceps* with rocky habitats versus the generalist habitat use of *H. binoei*, we expected to uncover finer-scale phylogeographical structure in the former because of dispersal limitation. We then overlay comparisons of multivariate morphology and chemical composition of epidermal pore secretions (chemical signals) to examine how differentiation across multiple dimensions plays out in the two codistributed species complexes. Given recent results from eastern *H. binoei* (Zozaya et al., 2019), the putative role of epidermal pore

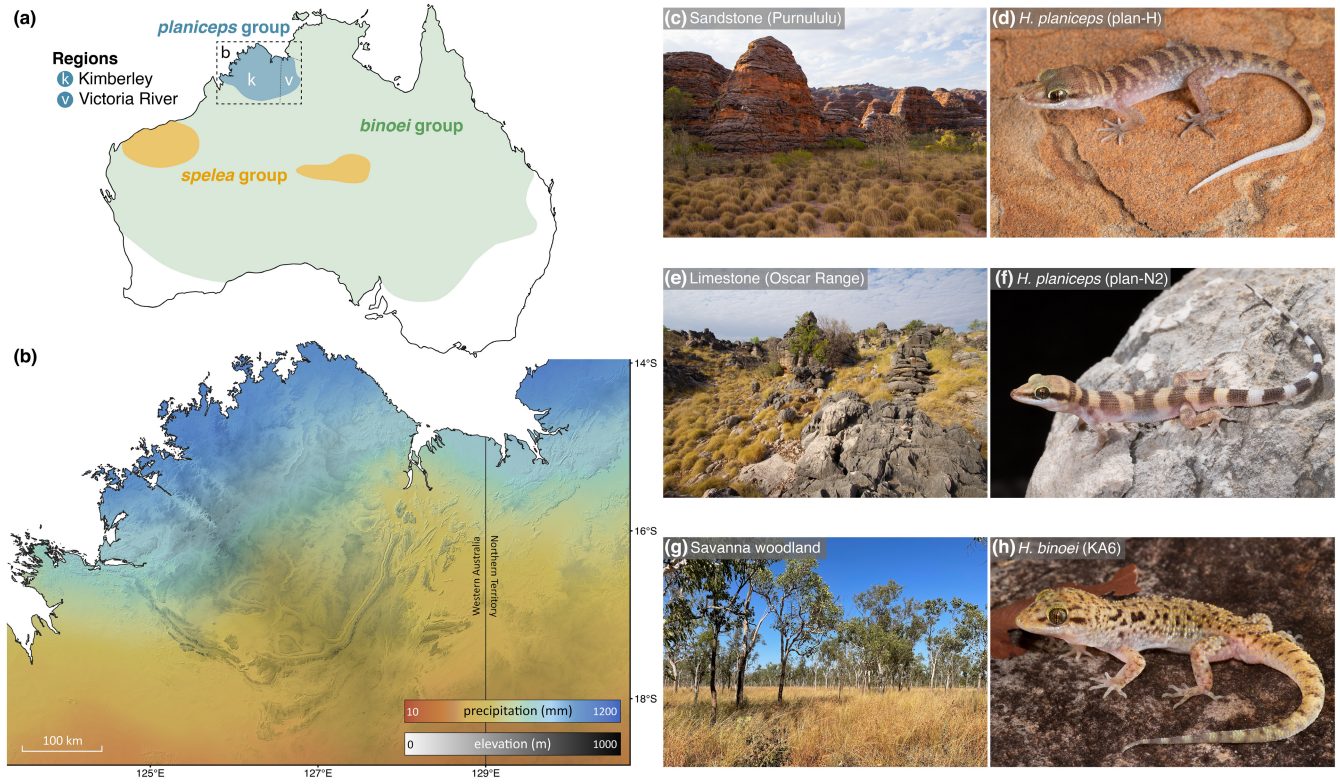


FIGURE 1 (a) Distributions of the three species groups within *Heteronotia* geckos (note that *Heteronotia binoei* occurs across the distributions of the other species groups). (b) The area of focus in this study, showing the Kimberley and Victoria River regions. A red–blue colour gradient illustrates variation in mean annual precipitation from the mesic north to the arid south, with hill-shading and a greyscale elevation gradient used to illustrate topographic complexity. (c–h) Examples of different habitats and their associated *Heteronotia* geckos: (c) sandstone gorges of the Purnululu massif and the (d) *Heteronotia planiceps* plan-H lineage; (e) limestone karsts of the Oscar Range and the (f) *H. planiceps* plan-N2 lineage; (g) savanna woodlands of the mesic northern Kimberley and the (h) *H. binoei* KA6 lineage. Photo credits: (c–g) Stephen Zozaya; (h) Brendan Schembri.

secretions in behavioural isolation (Martín & López, 2014) and the generally higher lability of behavioural traits (Blomberg et al., 2003), we expected to observe stronger differentiation (i.e., less overlap in trait variation) in chemical signals versus morphology in both taxa.

## 2 | MATERIALS AND METHODS

### 2.1 | Approach

We first screened single-locus mtDNA diversity across *Heteronotia planiceps* and codistributed *Heteronotia binoei* to identify deeply divergent candidate lineages for further analysis. We then used exon-capture sequencing on a subset of samples from each candidate lineage, producing usable sequences for >500 nuclear DNA (nDNA) exons, with the added benefit of yielding multilocus mtDNA bycatch. Using these data, we then: (i) used nDNA to verify the monophyly of candidate lineages identified from single-locus mtDNA sequences; (ii) better estimated their phylogenetic relationships using concatenated and species-tree analyses; and (iii) estimated and compared levels of among-lineage genomic divergence. A stark case of phylogenetic incongruence among analyses then instigated a test for introgression between two geographically adjacent *H. planiceps* lineages. Following phylogenetic analyses, we then assessed and compared among-lineage differentiation for two phenotypic traits—ecomorphology and chemical signals—to explore whether divergence is proceeding in multiple dimensions. This included testing whether chemical signal composition has diverged more among lineages than has ecomorphology.

### 2.2 | Tissue sampling

Previous multilocus (one mtDNA + eight nDNA intron loci) sequencing of *H. binoei* revealed six independently evolving lineages overlapping the geographical range of *H. planiceps* (Moritz et al., 2016): four from the monsoonal tropics A6-2 clade (from east to west: NA6, VRD, KA6, NWK); and two widespread arid and semi-arid lineages (SM6N, SM6W). From these, we selected a geographically dispersed subset of individuals from each lineage for exon-capture sequencing ($N = 29$; Table S1). Our fieldwork greatly expanded the availability of tissues and specimens for *H. planiceps*, though gaps remain

in inaccessible regions. We note, based on multilocus sequencing, that many records of *H. planiceps* from more easterly localities (e.g., Arnhem Land in the Northern Territory) are instead strongly banded forms of *H. binoei* (Moritz et al., 2016). We sequenced all available *H. planiceps* tissues from the mainland, and representative island samples for mtDNA ($N$ = 168 individuals; Table S2) and, for exon capture, included 55 samples representing known mtDNA diversity and spanning the geographical range of *H. planiceps* (Figure 2b; Table S1). Finally, we also included eight samples representing diversity within the similarly rock-restricted *Heteronotia spelea* complex from the MacDonnell Ranges and Pilbara region of arid central and western Australia (Pepper et al., 2013; Figure 1a).

## 2.3 | Single-locus mtDNA sequencing and phylogenetics

New sequences for the 1041 bp mtDNA locus *NADH dehydrogenase subunit 2* (*ND2*) were obtained via PCR (polymerase chain reaction) and Sanger sequencing as described in Fujita et al. (2010) (followed by Moritz et al., 2016), but using newly developed primers to improve amplification success for *H. planiceps* (forward: 5′-GAGCCCCCTAATCTGAACAA-3′; reverse: 5′-TGTGGGGATAAG TGGTGATG-3′). The resulting 168 *ND2* sequences for *H. planiceps* (Table S2) were combined with the *ND2* alignment from Moritz et al. (2016)—pruned to retain only relevant lineages of

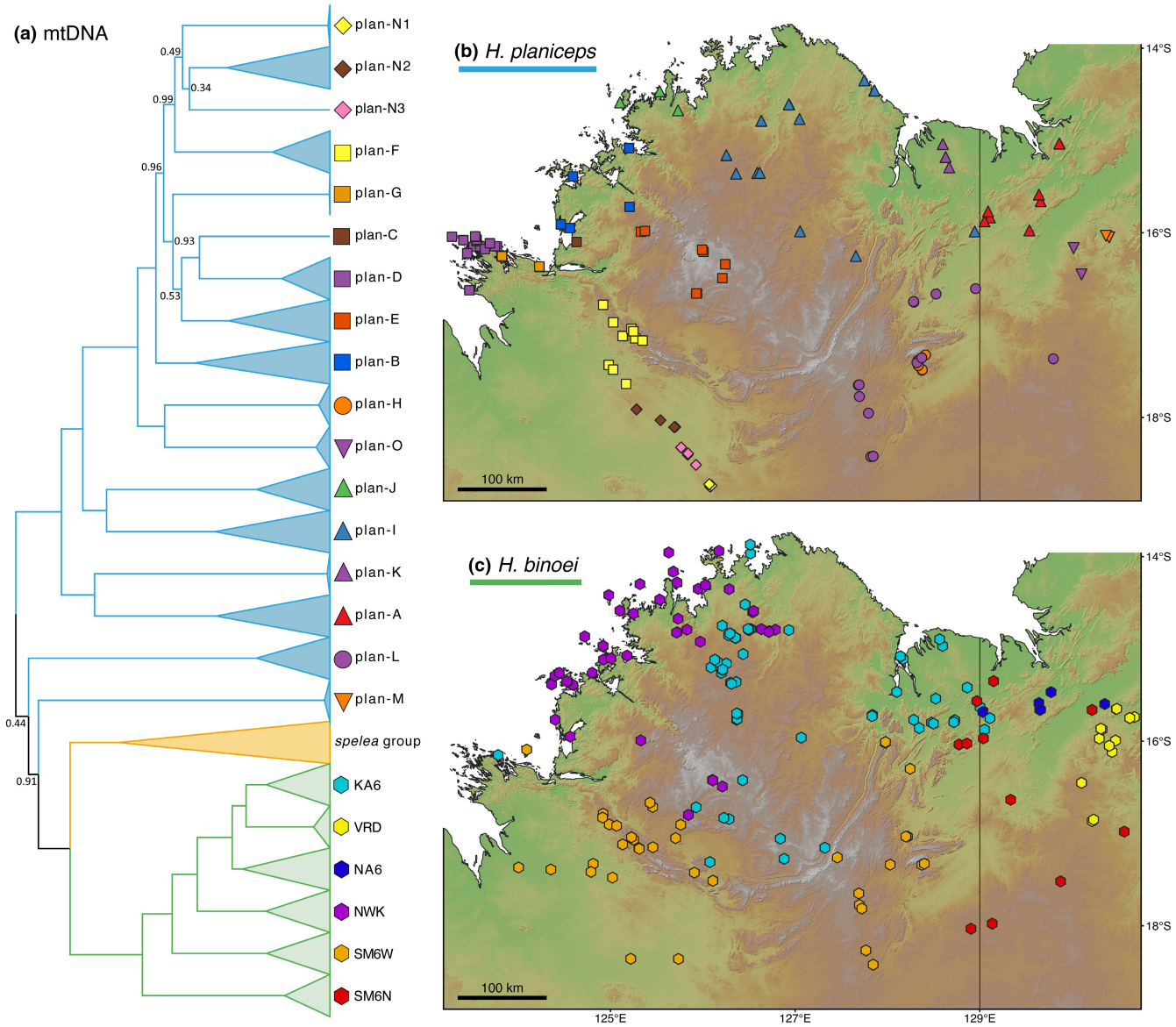


FIGURE 2 (a) Mitochondrial phylogeny of *Heteronotia* inferred using BEAST from 3843 bp across eight protein coding genes. Numbers on nodes indicate posterior probabilities <1. Shapes are unique to each lineage and correspond to maps (b, c) illustrating the distributions of all lineages within (b) *Heteronotia planiceps*, and then (c) lineages of *Heteronotia binoei* present in the Kimberley–Victoria River regions. Maps use hill-shading and an elevational colour gradient to illustrate topographic complexity. Note: The *Heteronotia spelea* group does not occur in the geographical range shown in (b, c) and so their sampling localities are not displayed in this figure.

*H. binoei*—yielding an alignment containing sequences from 633 individuals. Sequences were aligned using the default settings in GENEIOUS PRIME version 2021.2.2 followed by visual inspection, including amino acid translation to check for unexpected stop codons and frame shifts. We then performed phylogenetic analysis of *ND2* sequences via maximum-likelihood (ML) using IQ-TREE version 2.2.0 (Minh et al., 2020). The alignment was partitioned by codon, with MODELFINDER (Kalyaanamoorthy et al., 2017) used to determine the best substitution model. We executed 1000 ultrafast bootstrap replicates (implemented via UFBOOT2; Hoang et al., 2018), as well as branch support metrics via a Shimodaira–Hasegawa-like approximate likelihood ratio test (SH-aLRT; Guindon et al., 2010; Hoang et al., 2018) with 1000 replicates. We specified the GENESITE resampling strategy for the 512 concatenated exons, which is a two-step process that resamples partitions and then sites within partitions (Gadagkar et al., 2005; Seo et al., 2005), mitigating overestimates of bootstrap support (e.g., Roycroft et al., 2020). Phylogenetic analyses of multilocus mtDNA sequences obtained from exon capture bycatch are detailed below under "Phylogenomic estimation."

## 2.4 | Exon capture, mtDNA bycatch and bioinformatics

Details on the design of our exon capture system are identical to those presented in Zozaya et al. (2022a). Briefly, following Bi et al. (2012) we designed a custom exon capture system using de novo assembled adult liver transcriptomes obtained from individuals of three lineages of *H. binoei* (NWK, VRD, SM6N) and one of *H. planiceps* (plan-A), as outlined in Zozaya et al. (2022a). Following the strategy in Bragg et al. (2016), we targeted 4406 protein-coding exons longer than 200 bp and represented just once in the *Anolis* genome (Alföldi et al., 2011). Custom probes were synthesized using the Nimblegen SeqCap EZ system. Individually indexed genomic libraries were prepared following Meyer and Kircher (2010) as modified by Bi et al. (2012), enriched for target exons by hybridization as in Potter et al. (2018), and sequenced (100 paired-end) on an Illumina HiSeq 2000 platform. We processed raw sequencing reads following the pipeline presented in Bragg et al. (2016)—and similarly followed by Moritz et al. (2018) and Ashman et al. (2018). This pipeline uses the read-backed phasing tool in GATK (release gb82c674, McKenna et al., 2010) to identify heterozygous sites and perform haplotype phasing. This produces two haplotypes for each locus, referred to here as h0 and h1. Of these, the h0 haplotype consists of the more frequent allele in the reads and is, therefore, less likely to be influenced by cross-contamination. Further details for *Heteronotia* exon capture are outlined in Zozaya et al. (2022a). After data assembly and filtering, we recovered an average of 2002 loci with mean coverage >20× (0.97 Mb) and overall mean coverage of 48× for the 33 *H. binoei* samples and 1429 loci with mean coverage >20× (0.89 Mb) and overall mean coverage of 34× for the 46 *H. planiceps* samples.

Assembled haplotypes were aligned using MACSE (Ranwez et al., 2011) to ensure alignments were in the correct reading frame. Exons were ranked by the number of variable sites, followed by visually checking those with the highest number of variable sites as this can indicate misalignment, contamination or paralogous sequences. We removed alignments less than 150 bp in length (as a proxy for information content), and then removed alignments containing fewer than 90% of sequenced individuals. This yielded a highly complete data set of 512 exon loci for subsequent analysis. Finally, alignments were trimmed using BMGE (Criscuolo & Gribaldo, 2010), followed by manual inspection of each alignment to check that reading frames were correct and that no stop codons were present within exons.

We assembled mtDNA bycatch from exon capture with MITOBIM (Hahn et al., 2013), using a previously published reference mitochondrial genome of *H. binoei* to seed the assembly (GenBank accession EF626807; Fujita et al., 2007). We then mapped the reads for each individual back to its own MITOBIM assembly and corrected incorrectly incorporated sequencing errors using the majority call for each base. Regions with a read depth of less than 20 were then hard masked. The final assemblies were then aligned using MAFFT (Katoh et al. 2002 ) and we manually trimmed regions composed mostly of gaps and ambiguities, as well as tRNA regions that were very difficult to align. This left 3843 bp covering all or parts of eight protein coding genes: *COX1* (partial: 726 bp), *COX2* (687 bp), *ATP8* (partial: 129 bp), *ATP6* (678 bp), *COX3* (783 bp), *NAD3* (345 bp), *NAD4L* (633 bp) and *ND4* (partial: 207 bp). The final alignment was manually checked against the reference genome to ensure it was in the correct reading frame, with no unexpected stop codons or frame shifts.

## 2.5 | Phylogenomic estimation

We first performed two ML phylogenetic analyses via IQ-TREE version 2.2.0 (Minh et al., 2020): one on the multigene mtDNA bycatch, and the other on the concatenated set of 512 exons (h0 haplotype) for all individuals. Each analysis was partitioned by locus (Chernomor et al., 2016) with MODELFINDER (Kalyaanamoorthy et al., 2017) used to determine the best substitution model for each locus. As for the *ND2* sequences, we again executed 1000 ultrafast bootstrap replicates and branch support metrics via SH-aLRT with 1000 replicates. For the 512 concatenated exons, we again specified the GENESITE resampling strategy. For the mtDNA bycatch, we then ran a Bayesian phylogenetic analysis using BEAST2 (Bouckaert et al., 2014). We partitioned sequences by gene and used the GTR+Γ (four gamma categories) model for each partition. We used the Yule model for the tree prior, and uncorrelated branch rates (mean = 1) sampling from an exponential distribution. The analysis was run for 10,000,000 generations with a 20% burn-in and sampling trees every 1000 generations.

For species tree analyses, we first estimated relationships using the quartet-based algorithm implemented in ASTRAL-III version 5.7.8 (Zhang et al., 2018). To do this, we first produced individual gene trees for each of our 512 exon alignments using IQ-TREE version 2.2.0. MODELFINDER was used to determine the substitution model for each gene, and support values for branches within each gene

tree were estimated with 100 nonparametric bootstrap replicates (Felsenstein, 1985). We also performed Bayesian multispecies coalescent phylogenetic analysis using STARBEAST2 version 0.13.1 (Ogilvie et al., 2017) implemented in BEAST2 (Bouckaert et al., 2014). Given computational constraints, we selected the 100 exons that are most completely represented across the identified lineages, selecting one or two samples per lineage (some lineages are represented by only a single sample; e.g., plan-C, plan-N3). The analysis was run with a partition for each exon and GTR+Γ site model for each exon, with four Γ categories and using empirical rate frequencies. We used a strict clock model and a birth–death tree prior. We ran two independent instances of the analysis until all effective sample size (ESS) values exceeded 200 (just over 2 billion generations) and checked for convergence between the two runs in TRACER version 1.7 (Rambaut et al., 2018). We then built a Maximum Clade Credibility tree using TREEANNOTATOR with common ancestor node heights and a 10% burn-in.

## 2.6 | Post hoc test for introgression

Given incongruences among species tree reconstructions with strong statistical support, we performed two hypothesis-based, post hoc tests for introgression: one from plan-H to plan-L within *H. planiceps*, and the other from KA6 to NWK within *H. binoei*. As these analyses are based on the results of our planned phylogenetic analyses, the justification for these tests is detailed more fully in the respective Results section. Briefly, unidirectional introgression from plan-H to plan-L was tested based on the deeply divergent placement of plan-L in the IQ-TREE and ASTRAL-III reconstructions (as well as all mtDNA analyses), vs. a close sister relationship to plan-H in the STARBEAST2 reconstruction (see "Results"). Unidirectional introgression from KA6 to NWK was also tested based on the NWK lineages being sister to the clade containing KA6, NA6 and VRD in all phylogenetic reconstructions except the STARBEAST2 species tree, and previous findings of extensive unidirectional mtDNA introgression from KA6 to NWK (Moritz et al., 2016). We tested for introgression using the multispecies-coalescence-with-introgression (MSCi) analysis in BPP version 4.4.0 (Flouri et al., 2020). This was done using the same 100 exon loci used in the STARBEAST2 analysis. To reduce computation time, only five lineages were included in the analysis of *H. planiceps* (plan-M, L, I, H, F) and only four lineages for *H. binoei* (SM6W, NWK, VRD, KA6). Fixed topologies among lineages were specified based on the 512 exon IQ-TREE and ASTRAL-III reconstructions for each analysis. The topology for *H. planiceps* was specified as: (plan-M, (plan-L, (plan-I, (plan-H, plan-F)))). The topology for *H. binoei* was specified as: (SM6W, (NWK, (KA6, VRD))). Priors were specified for *theta* (=0.003 e) and *tau* (=0.003) for both analyses following estimation from a preliminary A0 analysis. Hybridization nodes along branches leading to plan-H or KA6 (node X) and plan-L or NWK (node Y) were specified for each, with the prior introgression probability φ from X to Y specified as .01 for the first run and .10 for the second run to ensure similar posterior φ estimates with varying priors. Analyses were each run with a burn-in of 1000,000 generations and a sampling frequency of 10 for a total of 1000,000 samples in the posterior distribution (11,000,000 total generations). Parameter convergence was confirmed using TRACER version 1.7.2 (Rambaut et al., 2018).

## 2.7 | Nucleotide divergence

Estimates of between-lineage nucleotide diversity were calculated using *PopGenome* version 2.7.5 (Pfeifer et al., 2014) in R version 4.0.3 (R Core Team, 2020). Metrics were estimated separately for the *H. binoei* and *H. planiceps* groups. We estimated absolute ($D_{xy}$) and net ($D_a$) nucleotide divergence between lineages (Nei, 1973; Nei & Li, 1979). This was first estimated across all sites, then again across only synonymous (3rd codon) sites to compare how divergence falls along the "grey zone" of speciation (0.5%–2% synonymous $D_a$) as identified by Roux et al. (2016). In all cases, we included nucleotide positions with missing data when reading alignments into *PopGenome*. Designations of individuals to a lineage were based on phylogenetic analyses of mtDNA and nDNA, which indicated that all putative lineages are monophyletic (see "Results"). Estimates of mtDNA nucleotide diversity were done across the 3843-bp alignment obtained from exon capture bycatch. Mitochondrial bycatch was successful for only a single sample from each of plan-C, plan-N3 and plan-O. These lineages were therefore excluded for mtDNA as this precludes estimates of within-lineage diversity necessary to calculate $D_a$. Estimates of nDNA nucleotide diversity were done across 507 exon loci using both haplotypes (h0 and h1) from each individual. Five of the original 512 loci subsets were excluded because of errors that aborted analyses when included, the cause of which could not be resolved. $D_{XY}$ and $D_a$ were estimated for each locus and then averaged across the 507 loci. Samples from individuals with >10% ambiguous sites for nDNA were excluded, including the sole sample for the plan-N3 lineage (~70% ambiguities).

## 2.8 | Morphology

We collected morphometric data from ethanol-preserved museum specimens representing 16 genetic lineages of *H. planiceps* ($N = 95$; 1–18 per lineage; mean = 6) and the six co-occurring lineages of *H. binoei* ($N = 84$; 5–19 per lineage; mean = 14). Nine linear measurements were done to the nearest 0.1 mm using a Mitutoyo digital calliper. These measurements were: snout-to-vent length (SVL), from the anterior tip of the rostral scale to the posterior margin of the cloaca; head length (HL), from the anterior tip of the rostral scale to the anterior margin of the ear; head width (HW), the widest point on the head, just anterior to the ears; head depth (DP), maximum depth of head just posterior to the orbitals, measured transversely; interlimb length (ILL), from the posterior insertion of the forelimb to the anterior insertion of the hindlimb; forelimb length (FLL), the elbow to the wrist with the upper arm and wrists held at right angles to the forearm; hindlimb length (HLL), the knee

to the ankle with the upper leg and ankle held at right angles to the lower leg; orbit length (OrbL), measured horizontally from the anterior to the posterior margins of the orbit; and snout length (SnEye), the anterior tip of the rostral scale to the anterior margin of the orbit. See Table S3 for raw data. For comparisons of body size divergence among lineages in *H. planiceps* (see post hoc analysis under "Phenotypic analyses" below), we also supplemented these morphometric data with additional SVL measures from live, wild individuals due to the low number of preserved specimens for some lineages (Table S4). This was done using a transparent plastic ruler with the gecko held flat against it and with the body straight, with measures taken to the nearest millimetre.

### 2.9 | Epidermal pore secretions (chemical signals)

We used data from Zozaya et al. (2022b) to assess how among-lineage divergence in a chemical signalling trait (male epidermal pore secretions) compares to morphological divergence among lineages in each of the two species groups. Chemical data were available for the six relevant lineages of *H. binoei*, but only eight lineages of *H. planiceps*: plan-A, plan-I, plan-J, plan-L, plan-M, plan-N1, plan-N2 and plan-N3. While this is only a subset of the lineage diversity present in *H. planiceps*, it spans the phylogenetic breadth of the complex (see "Results"). All details on the collection and chemical characterization of epidermal pore secretions are presented in Zozaya et al. (2022a). Briefly, secretions are collected from the precloacal epidermal pores of male geckos (only male *Heteronotia* possess these pores), followed by storage at −20°C, and characterization via gas chromatography (GC). A total of 29 chromatogram peaks were used, with each peak representing a compound or several compounds with identical retention times (see Zozaya et al., 2022a). The relative proportion of each peak was calculated by dividing the area under the respective peak by the sum of the area under all 29 peaks (total ion current) for the respective sample. Finally, each peak was then logit-transformed to account for the unit-sum constraint of proportions (Aitchison, 1986; Warton & Hui, 2011).

### 2.10 | Phenotypic analyses

Following the approach of Zozaya et al. (2019) on eastern lineages of *H. binoei*, we tested whether lineages within each of the two species groups differed more in morphology or the chemical composition of epidermal pore secretions. For *H. planiceps*, we restricted our analyses to the seven lineages represented by both morphometric and chemical data sets (data for all six *H. binoei* lineages were available). We first performed principal components analyses (PCA) separately on morphology (nine variables) and chemical signals (29 variables) using the "rda" function in the R package *vegan* (Oksanen et al. 2017), with a correlation matrix specified so that all variables were scaled (Jolliffe et al., 2007). We plotted PC1 and PC2 for each trait to visualize phenotypic variation within and among lineages.

We used a distance-based approach to compare levels of trait divergence, rather than trait space overlap (e.g., Zozaya et al., 2019), because of the small sample sizes for some lineages (which complicates estimating trait space, e.g., convex hull polygons). Using PC1–5 for each trait, we calculated the Euclidean distance between every point using the "vegdist" function in *vegan*, and then averaged distances between each lineage pair (mean pairwise distance) using the "meandist" function (Oksanen et al., 2017). For *H. planiceps*, PC1–5 accounted for 95% of morphometric variation and 79% of chemical signal variation; for *H. binoei*, PC1–5 accounted for 95% of morphometric variation and 64% of chemical signal variation. Finally, we tested whether morphology or chemical signals have diverged to a greater degree among lineages using a *t*-test, with mean pairwise trait distance as the response variable and trait type as the explanatory variable.

Based on the results from the above analysis, we performed an exploratory, post hoc test to assess whether larger body size is associated with specialization to limestone habitats (see "Results" for further details). We calculated average SVL for each of 14 lineages of *H. planiceps* represented by two or more adult individuals (including measures of both preserved specimens and field-measured individuals to increase sample sizes; Table S4), and then tested whether body size is associated with rock type (limestone/sandstone) using phylogenetic generalized least squares regression. The IQ-TREE phylogeny of 512 concatenated exons (see "Results") was used for analysis, retaining one tip per lineage. We did this twice—one modelling a Brownian motion (BM) model of trait evolution, the other modelling an Ornstein–Uhlenbeck (OU) process—and then compared models using Akaike's information criterion (AIC).

## 3 | RESULTS

### 3.1 | mtDNA phylogeography

Increased sampling in the Kimberley region increased the spatial density of *Heteronotia binoei* samples, but did not reveal any additional lineages or appreciably extend the known ranges of the six major lineages described in Moritz et al. (2016) (Figure 2a,c; Figure S1). These lineages are largely parapatric, with rare instances of sympatry at geographical boundaries: NWK and KA6 in the north and central-west Kimberley; SM6W, KA6 and NA6 in the eastern Kimberley; and SM6N, VRD and NA6 in the Victoria River region (Figure 2c). The SM6W, SM6N and NA6 lineages each have ranges extending well beyond the study region: SM6W southwards across the western and central arid zone; SM6N eastward across northern Australia into northwestern Queensland; and NA6 eastwards across the Top End of the Northern Territory. Introgression of KA6 mtDNA into NWK individuals (as identified by morphology and nDNA introns; Moritz et al., 2016) is known for some northwest Kimberley populations, but has not been recorded elsewhere, or among other lineages in the region.

Based on our extensive mtDNA *ND2* sequencing, we grouped diversity within *Heteronotia planiceps* into 17 monophyletic, candidate lineages (Figure 2a; Figure S1), although some of these contain further deep internal structure: plan-A and plan-I from the north and east Kimberley, and plan-E and plan-B from the mesic northwest Kimberley. Notably, the rock-associated *H. planiceps* exhibits a much finer-scale and deeper phylogeographical structure than is the case for the habitat generalist *H. binoei* (Figure 2b). In fact, the mtDNA BEAST phylogeny recovers the divergent plan-M and plan-L lineages as allied to the clade containing the *H. binoei* and *Heteronotia spelea* complexes (albeit with low support; Figure 2a), rendering *H. planiceps* paraphyletic. This same topology is observed when the maximum-likelihood IQ-TREE is midpoint rooted (Figure S1). While short internode lengths, low statistical support and results from nDNA exons (below) indicate this deep topology is inaccurate, it highlights the remarkable levels of mtDNA divergence within *H. planiceps* across a modest distribution compared to other clades of *Heteronotia*.

The deepest branching lineages occur in the east (plan-L, plan-M) and north Kimberley (plan-A + plan-K as one clade, plan-I + plan-J as another). The nine lineages from the western Kimberley form a clade, within which relationships are poorly resolved. Three of these are endemic to disjunct limestone ranges in the otherwise arid southern Kimberley. Sister to these west Kimberley lineages is a clade with two geographically restricted lineages from the southeast Kimberley. The latter, plan-H and plan-O, occur in sandstones of the Purnululu massif and Victoria River region, respectively, adjacent to the highly divergent plan-L and limestone-restricted plan-M lineages (Figure 2b).

The small geographical scale of lineage diversity exhibited by the *H. planiceps* complex is striking compared to codistributed lineages of *H. binoei* (Figure 2b,c; Table S5). Lineages of *H. planiceps* tend to have very small distributions (using minimum convex polygons; mean = 5560 $km^2$, median = 968 $km^2$), with only two lineages exceeding 10,000 $km^2$: plan-I (38,353 $km^2$) in the lower relief northeast Kimberley, and plan-L (27,305 $km^2$) in the semi-arid southeast Kimberley and southern Victoria River basin. Eight of the 17 lineages of *H. planiceps* have estimated distributions less than 100 $km^2$ (Table S5), with the smallest being the limestone-restricted plan-M lineage at ~9 $km^2$ (excluding plan-C, which is known from only a single site). This is in stark contrast to the distributions of regional *H. binoei* lineages, which have much larger distributions (mean = 473,756 $km^2$, median = 122,961 $km^2$). Only the VRD lineage at 11,983 $km^2$ has a distribution size within the range observed for *H. planiceps*. By comparison, the three *H. binoei* lineages extending beyond the Kimberley–Victoria River regions have extremely large distributions: NA6 at 153,539 $km^2$, SM6N at 585,631 $km^2$ and SM6W at 1,947,671 $km^2$.

## 3.2 | Phylogenomic reconstructions

For the nDNA exons, the concatenated IQ-TREE analysis and both the ASTRAL and STARBEAST2 species trees recover *H. binoei* as sister to the clade containing the *H. planiceps* and *H. spelea* complexes, with the latter two being sister to each other (Figure 3; Figures S2 and S3). All lineages as defined by mtDNA and with multiple individuals (thus excluding plan-N3 and plan-C, each $N = 1$) were strongly supported as monophyletic (bootstrap support [BS] ≥ 96; aLRT ≥98) in the concatenated IQ-TREE analysis (Figure S2). The ASTRAL analysis (Figure S3) similarly recovered most candidate lineages as monophyletic with full support, with the exceptions of plan-B (posterior probability [pp] = 0.51; although with strong support for the clade containing plan-B and the closely related plan-C [pp = 0.96]) and plan-F (pp = 0.63). Collectively, these observations of nDNA monophyly give confidence that each of the major mtDNA clusters represents a distinct evolutionary lineage, rather than a single locus artefact.

In general, the nDNA phylogenies for *H. planiceps* present the same major geographical patterns as for mtDNA, with the deepest branching lineages in the east and north, and a well-supported clade of lineages in the west. In detail, both the concatenated IQ-TREE (Figure 3a) and ASTRAL (Figure S3) species tree accord with the mtDNA topology in having east Kimberley plan-M and plan-L lineages as the deepest branches, followed by north Kimberley lineages (plan-A, I, K, J), then east Kimberley sandstone taxa (plan-O, plan-H), and, finally, the clade containing west Kimberley lineages. For the STARBEAST2 species tree, there is congruence with previous analyses for *H. planiceps* in that plan-M is again sister to the remainder of *H. planiceps*, north Kimberly lineages are deep in the tree, and congruent relationships are found among the west Kimberley lineages. There is, however, incongruence among phylogenies in the placement of the southeast Kimberley plan-L; in all other analyses for mtDNA and nDNA loci, this lineage is the second deepest branching in *H. planiceps*, whereas in the STARBEAST2 analysis it clusters strongly with the geographically adjacent plan-H. This is not an artefact of the 100 loci selected for the STARBEAST2 analysis, as a concatenated ML tree for the same set loci again places plan-L as the second deepest branching lineage, distant from plan-H which again is sister to the west Kimberley clade (Figure S4; we return to this case of incongruence below). While there are several other instances of potential incongruence among trees—particularly for the north Kimberley lineages (Figure 3)—these appear to reflect phylogenetic uncertainty and are often associated with short and poorly supported internode branches, as would be expected of a recent and rapid radiation.

All analyses differed somewhat in their support for relationships within the *H. binoei* lineages included herein. All nDNA analyses agreed that the SM6N and SM6W lineages form a clade sister to the remaining four lineages (the A6-2 clade; Moritz et al., 2016: NWK, KA6, NA6, VRD), although mtDNA does not support a sister relationship between SM6N and SM6W (Figure 2a; see also Fujita et al., 2010). Relationships within the A6-2 clade vary with each analysis, with mtDNA and the 512 exon IQ-TREE and ASTRAL phylogenies all supporting a topology where NWK is sister to the remaining three, whereas the STARBEAST2 species tree strongly supports a sister relationship between the geographically adjacent NWK and KA6 lineages. Notably, mtDNA introgression from KA6 into NWK has been recorded previously (Moritz et al., 2016). Internode lengths are short

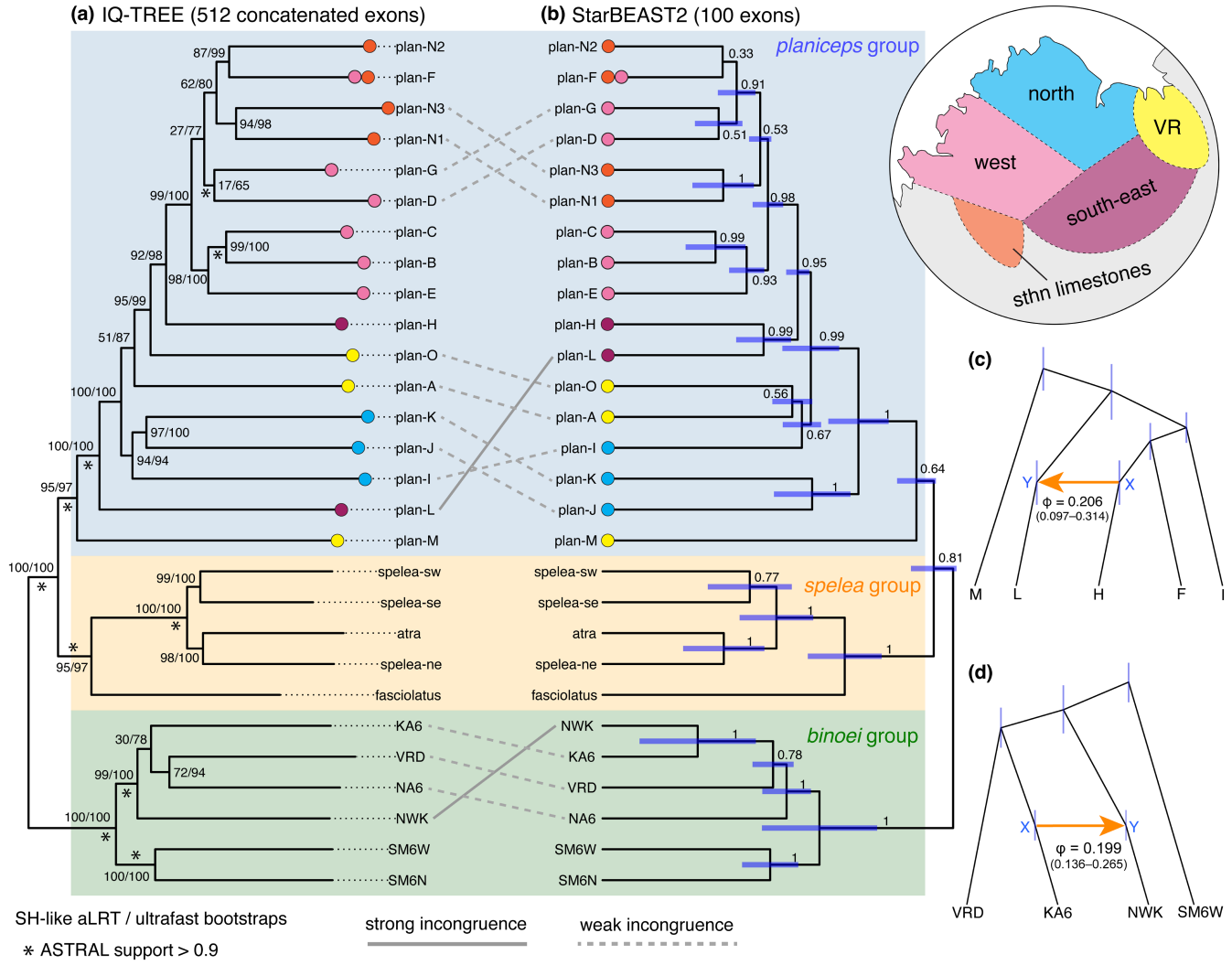


FIGURE 3 Phylogenies of *Heteronotia* comparing the (a) concatenated 512 exon IQ-TREE phylogeny (pruned to show a single tip per lineage; see Figure S2 for full tree) and (b) 100 exon STARBEAST2 phylogeny. Relationships in the concatenated tree (a) with high corresponding support (pp >0.9) in the ASTRAL-III species tree (Figure S3) are shown with an asterisk. Grey lines connect incongruent lineage placements between phylogenies: Dashed lines indicate incongruence associated with low statistical support (weak incongruence), while solid lines indicate incongruence associated with strong support in both trees (strong incongruence). Coloured dots at tips of *Heteronotia planiceps* lineages reflect the geographical areas portrayed on the top-right (VR = Victoria River region). The phylogenetic networks (c, d) show results from introgression tests done via the MSCi analysis in BPP, which indicate historical introgression from (c) the ancestor of plan-H to the ancestor of plan-L, and (d) the ancestor of KA6 to the ancestor of NWK. The "plan-" prefix is not shown for lineages in (c) for graphical purposes.

within the A6-2 clade, reflected by generally low statistical support for bifurcations across the three nDNA phylogenies.

We return to the strongly supported incongruences between the STARBEAST2 species tree vs. all other analyses (mtDNA and nDNA) for the plan-L lineage of *H. planiceps* and the NWK lineage of *H. binoei*. (Other incongruent lineage relationships among trees had low statistical support in either one or more trees, and are not considered further here.) In most analyses, the plan-L lineage is consistently recovered as the second deepest branching event in the *H. planiceps* complex, and the *H. binoei* NWK lineage is recovered as sister to the clade containing the KA6, NA6 and VRD lineages. In the STARBEAST2 tree, however, plan-L is nested deeply in the phylogeny with a sister relationship to plan-H, and NWK is recovered as the closely related sister lineage to KA6. One possible cause of these incongruences is incomplete lineage sorting (ILS), which is not accounted for in the concatenated IQ-TREE reconstruction. The ASTRAL-III reconstruction, however, does account for ILS and is congruent with both mtDNA and concatenated exon analyses with respect to these lineages. In addition, while methodological artefacts of the STARBEAST2 analysis cannot be ruled out, both cases of incongruence involve parapatric lineages that occur at the scale where individuals might meet and mate in the wild (Figure 2). Furthermore, unidirectional mitochondrial introgression from KA6 to NWK has been found in a previous study (Moritz et al., 2016). We thus consider introgression, a serious model violation, as a possible cause of incongruences between the full Bayesian analysis and other approaches.

We performed post hoc tests for introgression to explore this possibility using the MSCi analysis in BPP version 4.4.0 (Flouri

et al., 2020; see "Methods"). This test estimated an introgression probability φ = 0.206 (highest posterior density [HPD] credibility interval φ = 0.097–0.314) from the ancestor of plan-H to the ancestor of plan-L (node X to Y; Figure 3c). This test also estimated an introgression probability φ = 0.119 (HPD credibility interval φ = 0.199–0.265) from the ancestor of KA6 to the ancestor of NWK (node X to Y; Figure 3d). These results were each consistent across two runs of the analysis with different φ priors. Because the HPD intervals do not include 0.001, we follow Ji et al. (2021) in considering each of these results as strong evidence of historical introgression between the respective lineages.

### 3.3 | Genetic divergence among lineages

We estimated and compared sequence divergence for mtDNA and nDNA exons among lineages within each of the two species groups. The upper estimates of mtDNA sequence divergence in *H. planiceps* were similar to or, for net values, greater than those observed in Kimberley lineages of *H. binoei* (Table S6). Absolute mtDNA divergences up to 9.3% $D_{xy}$ were observed within *H. planiceps* vs. 8.4% $D_{xy}$ within *H. binoei*; net divergences up to 8.6% $D_a$ were observed within *H. planiceps* vs. 6.3% $D_a$ within *H. binoei*. Absolute synonymous divergence (i.e., at 3rd codon positions) was similar between the two species groups, being slightly higher in *H. binoei* (max. 16.2% $D_{xy}$ in *H. planiceps* vs. 16.6% $D_{xy}$ in *H. binoei*), but net synonymous divergence was again higher in *H. planiceps* (max. 15.5% $D_a$ in *H. planiceps* vs. 12.4% $D_a$ in *H. binoei*).

Across the 507 nDNA exons, maximum divergences within *H. planiceps* also exceeded those among Kimberley lineages of *H. binoei* (Table S7). Absolute divergences up to 1% $D_{xy}$ were observed within *H. planiceps* versus 0.91% $D_{xy}$ within *H. binoei*; net divergences up to 0.78% $D_a$ were observed within *H. planiceps* vs. 0.54% $D_a$ within *H. binoei*. Absolute synonymous divergence (i.e., 3rd codon positions) up to 2.25% were observed within *H. planiceps* vs. 2.12% $D_{xy}$ within *H. binoei*; net synonymous divergence among lineages ranged from 0.87 to 1.06% $D_a$ within *H. binoei*, and from 0.37% to 1.76% $D_a$ within *H. planiceps*. We highlight that, for both *H. binoei* and *H. planiceps*, these net synonymous $D_a$ values span the "grey zone" of speciation (0.5%–2% net synonymous $D_a$) as recognized by Roux et al. (2016).

### 3.4 | Phenotypic differentiation

*Heteronotia binoei* is an ecological generalist that occurs in grasslands and woodlands across a variety of substrate types in addition to rocky areas. In contrast, *H. planiceps* is restricted to rocky substrates but occurs on all major rock types of the Kimberley region: sandstones, granites, basalt and limestones. While several lineages of *H. planiceps* are restricted to limestone (plan-M, plan-N1, N2, N3), the remainder all occur on sandstones to at least some degree; even if they are also found on granites and limestones (e.g., plan-F, plan-L). Of note is habitat separation of geographically proximal lineages. At Purnululu National Park, plan-H occurs on the sandstone massif (Figure 1b), while plan-L occurs on a narrow band of limestone immediately adjacent to the sandstone (but is on various rock types elsewhere). Similarly, in the Victoria River region, the highly divergent plan-M is known only from two adjacent limestone outcroppings, whereas plan-O occurs in sandstone gorges nearby.

Multivariate morphological variation among lineages is limited and largely overlapping in both *H. binoei* (Figure 4a) and *H. planiceps* (Figure 4b), with most among-lineage differentiation represented by body size (i.e., PC1). Body size divergence in *H. planiceps*, however, suggests the possibility that limestone-restricted lineages are larger (e.g., plan-M, plan-N1, N3; examined in more detail below). In contrast to morphology, and in line with our predictions, chemical signal divergence in both species complexes appears more pronounced among lineages (Figure 4c,d). Indeed, our comparison of differentiation across the two traits shows that chemical composition has diverged more among lineages than has morphology in both *H. binoei* (*t* test: $df = 27.9$, $t = 12.99$, $p < .001$) and *H. planiceps* (*t* test: $df = 31.4$, $t = 4.45$, $p < .001$). In *H. binoei*, mean among-lineage pairwise Euclidean distance for chemical composition (2.549) was 1.5 times greater than mean among-lineage pairwise distance for morphology (1.697). In *H. planiceps*, mean among-lineage pairwise Euclidean distance for chemical composition (2.772) was 1.32 times greater than mean among-lineage pairwise distance for morphology (2.101). Inspection of chemical signal variation in *H. binoei* (Figure 4c) shows that, while divergence is nevertheless greater than morphology, there is still considerable overlap in variation among lineages (with the exception of the extremely widespread and arid SM6W lineage). In contrast, there is much less overlap in chemical variation among lineages of *H. planiceps* (Figure 4d), with notable differentiation between the southwestern limestone lineages (plan-N1, N3) and remaining lineages.

Finally, using a post hoc exploratory analysis, we tested whether the limestone-restricted lineages of *H. planiceps* are larger (greater SVL) than the sandstone/rock-generalist lineages using phylogenetic generalized least-squares regression. Fourteen *H. planiceps* lineages had SVL measures from two or more adult individuals and were included in the analysis (plan-C and plan-K were excluded). Of these 14 lineages, four were regarded as limestone-restricted (plan-M, N1, N2, N3) and the rest were considered as sandstone/rock generalists. Limestone-restricted lineages are, on average, 3.2 mm larger when considering a BM model of trait evolution ($F_{1,12} = 7.19$, $p = .019$), and 3.5 mm larger when considering an OU model ($F_{1,12} = 12.73$, $p = .004$) (Figure 4c). The BM model had a lower AIC score (58.3) than the OU model (59.8), although scores are very similar and could be considered equivalent (ΔAIC = 1.5). Nevertheless, both models suggest that limestone-restricted lineages are significantly larger than sandstone/rock-generalist lineages.

## 4 | DISCUSSION

Here we found that allopatric divergence—and thus the potential initiation of speciation—among the rock-dwelling lineages of *Heteronotia planiceps* is proceeding in multiple dimensions at a fine spatial scale: genomic divergence in allopatry, habitat specialization associated with modest morphological (body size) divergence, and

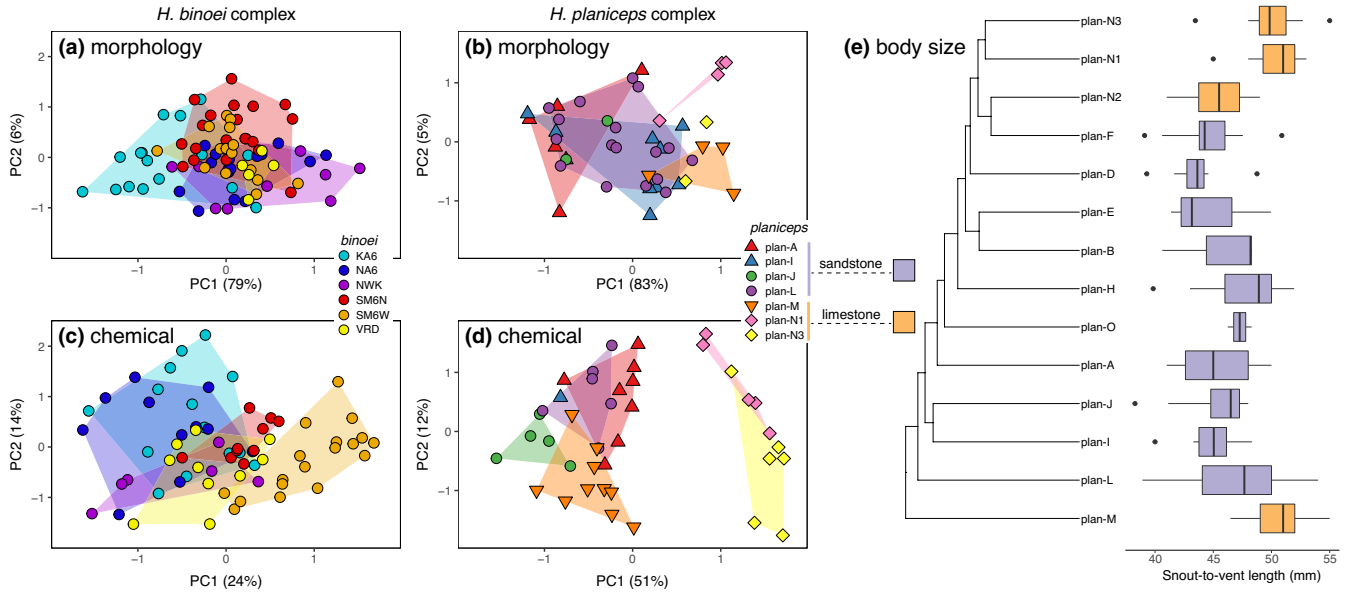


**FIGURE 4** Phenotypic variation among *Heteronotia* geckos in the Kimberley and Victoria River regions. Principal component (PC) axes illustrate trait variation for morphology within the (a) *Heteronotia binoei* and (b) *Heteronotia planiceps* groups, and then chemical signal variation within the (c) *H. binoei* and (d) *H. planiceps* groups (only seven lineages of *H. planiceps* had available data for both traits). In both species complexes, among-lineage trait divergence is greater for chemical composition than it is for morphology. (e) Body size variation (snout-to-vent length; SVL) with respect to phylogenetic relationships (IQ-TREE; 512 concatenated exons) across lineages of *H. planiceps*. Lineages restricted exclusively to limestone habitats (orange) are, on average, larger than those inhabiting sandstone and other rock types (purple) when accounting for phylogenetic nonindependence. Only the 14 lineages represented by two or more SVL measures from adult individuals are included.

relatively high differentiation in a chemical signalling trait (putative mating trait). Notably, among-lineage genetic divergence across the *H. planiceps* complex spans the "grey zone" of speciation (Roux et al., 2016), highlighting the suitability of this system for studying incipient speciation. In accord with expectations, both the diversity and geographical localization of lineages in *H. planiceps* far exceed that of its more ecologically generalist relative *Heteronotia binoei*, which itself has high levels of localized lineage diversity across other areas of the monsoonal tropics where *H. planiceps* is absent (Moritz et al., 2016; Zozaya et al., 2022a). Furthermore, the chemical composition of epidermal pore secretions differed more among lineages than did morphology in both species, and with clearer chemical signal divergence within *H. planiceps*. Among other lessons, our findings add to other studies suggesting that lizard taxa associated with rocky ranges and escarpments exhibit higher levels of phylogeographical structure and short-range endemism compared to taxa from surrounding grassland and woodland habitats (e.g., Laver et al., 2017; Oliver et al., 2019). Below we further discuss the genomic and phenotypic dimensions examined herein and how they might relate to the initiation—and possible completion—of speciation.

## 4.1 | Phylogeography and genomic divergence

Along with other rock-associated geckos in the Kimberley (*Gehyra*, Moritz et al., 2018; *Oedura*, Laver et al., 2017), *H. planiceps* shows highly localized phylogeographical structure. We identified a total of 17 lineages within *H. planiceps*, greatly expanding the lineage diversity uncovered in Pepper et al. (2011), which included only seven samples and identified four lineages across *H. planiceps*, and Oliver et al. (2017), which uncovered six deeply divergent genetic lineages but focused only on the western Kimberley. The level of lineage diversity exhibited by *H. planiceps* across such a relatively small region is exceptional, even exceeding that within the *Heteronotia spelea* complex, which is similarly rock-dwelling but spans a considerably larger area across the Australian arid zone (Figure 1). Indeed, lineage diversity in *H. planiceps* approaches the scale of short-range endemism observed in some groups of terrestrial snails in the Kimberley (Koehler, 2010). This is highlighted further by the lower level of phylogeographical structuring observed in the *H. binoei* complex, individuals of which are common in grassland and open woodland as well as rocky habitats—a pattern mirrored in rock-dwelling versus tree-dwelling *Gehyra* geckos in the region (Oliver et al., 2019). Pepper and Keogh (2014) suggested that geological heterogeneity of the Kimberley could affect diversification in low-dispersal species. For *H. planiceps*, the contrast between high lineage diversity and micro-endemism across the dissected sandstone formations of the west Kimberley versus a single widespread (plan-I) lineage across the gently sloping sandstone plateau of the northeastern Kimberley is consistent with this hypothesis. Additionally, there are highly restricted lineages in rocky refugia in the otherwise arid south and west Kimberley: deep sandstone gorges in Purnululu and the Victoria River region, and the disjunct Devonian limestones of the southern Kimberley and Victoria River region. This is again in contrast to a

widespread, rock-generalist (plan-L) distributed broadly across the topographically less complex southeastern Kimberley and southern Victoria River region.

The exceptionally deep and fine-scale phylogeographical structure within *H. planiceps* attests to high levels of population isolation and persistence across this rugged landscape. Population isolation was probably initiated by a combination of niche conservatism—with all lineages being rock specialists not found in open woodland—and the topographically complex geology of the region. Dispersal across nonrocky habitats may have been limited, setting the stage for simple allopatric divergence and accumulation of genetic incompatibilities (Avise et al., 1998; Wiens, 2004). This is consistent with the higher levels of nucleotide divergence observed among lineages of *H. planiceps* compared to the codistributed, ecologically generalist lineages of *H. binoei*. Nevertheless, levels of genomic divergence (0.37%–1.76% net synonymous $D_a$ in *H. planiceps* cf. 0.87%–1.06% in *H. binoei*) are below the level that alone suggests species status generally, including in lizards (Singhal & Moritz, 2013), and span the "grey zone" of speciation (0.5%–2% synonymous $D_a$) as identified by Roux et al. (2016). As such, it is likely that additional dimensions of reproductive isolation will influence possible outcomes of secondary contact, and thus the completion of speciation (Coyne & Orr, 2004).

## 4.2 | Phenotypic differentiation

Ecological divergence can mediate premating reproductive isolation by limiting how often individuals of different populations meet. Furthermore, phenotypic divergence resulting from adaptation to different environments (e.g., ecomorphology) can indirectly result in postzygotic isolation by rendering phenotypically intermediate hybrids unfit (Irwin & Schluter, 2022; Schluter, 2009). Ecomorphology is, in general, quite conservative within the *H. planiceps* complex, with the exception of larger body size in limestone-restricted lineages; but whether this reflects drift within isolates or habitat-induced adaptation is unclear and requires further investigation. Habitat separation (limestone vs. sandstone) of adjacent lineages in the east Kimberley and Victoria River regions is striking and suggests the possibility of habitat-driven ecological isolation, as has been implicated in other lizard groups in the region, such as *Gehyra* (Oliver et al., 2019) and *Cryptoblepharus* (Blom et al., 2016). The evidence for historical introgression inferred from plan-H (sandstone) to plan-L (limestone where it occurs near plan-H) suggests that, in this complex, ecological separation alone is not always sufficient. Even so, that the two lineages remain distinct in parapatry—occurring on adjacent but different rock types—suggests that some axis of differentiation has prevented the fusion of the two lineages despite historical introgression.

Whereas ecomorphological divergence among lineages was modest, we observed higher levels of among-lineage divergence in the chemical composition of male epidermal pore secretions, as was expected given the results of Zozaya et al. (2019). There is some evidence that epidermal pore secretions influence species discrimination and mate choice (Martín & López, 2014), including in geckos (Kabir et al., 2020). If this is also the case in *Heteronotia*, the divergence of chemical signals and associated mate preferences among lineages could result in behavioural (sexual) isolation (Coyne & Orr, 2004; Ritchie, 2007; Smadja & Butlin, 2009). This can contribute to the initiation of speciation when mating traits diverge among allopatric populations due to selection or drift, resulting in some degree of premating isolation upon secondary contact (Boughman, 2002; Hoskin et al., 2011; Lande, 1981).

In *H. planiceps*, the largest differences in chemical composition divide the limestone-dwelling lineages of the southern Kimberley (plan-N1–N3) from the remainder of *H. planiceps*. This divergence does not appear to result from occupying limestone environments per se (as is possibly the case for body size), as the limestone-specialist plan-M clusters with other, more rock-generalist lineages. Chemical signals vary in association with precipitation in *Heteronotia* (Zozaya et al., 2022a), and with temperature and other climatic factors in other lizards (Baeckens et al., 2018; Campos et al., 2020). As speculated in Zozaya et al. (2022a), the observed divergence may reflect the plan-N lineages (N1–N3) occupying the most arid regions, at the southern end of the distribution of the *H. planiceps* complex (and perhaps the divergent chemical blends observed here for the arid *H. binoei* SM6W lineage.) As we noted with regard to ecomorphological divergence, whether chemical divergence is a result of drift or selection cannot be determined. Mating signals can also evolve after other isolating barriers have arisen, for example, via selection for reproductive character displacement by reinforcement in the presence of strong postmating isolation (Butlin, 1987; Higgie et al., 2000; Hoskin et al., 2005; Howard, 1993; Noor, 1999). We note that reinforcement is unlikely to explain the pattern of chemical signal divergence observed herein, as the southern limestone lineages are geographically isolated from other populations of *H. planiceps*, and regional sympatry with *H. binoei* is ubiquitous across the distribution of *H. planiceps*. Given that prezygotic isolation, if stable (Seehausen et al., 2008), can take precedence over postzygotic incompatibilities (Coyne & Orr, 1989), more sampling of chemical signal divergence and its relation to mate choice at contact zones among lineages of *H. planiceps* could clarify premating isolating mechanisms in this complex, and—along with other codistributed lizard complexes (e.g., *Gehyra*)—is a promising area for further research in this rich Australian system.

## 4.3 | Concluding remarks and considerations

In sum, these new observations on genomic, ecological and phenotypic divergence among populations spanning the "grey zone" emphasize the multidimensionality of speciation. Whereas we tend to create dichotomies when debating the relative importance of one form of speciation over another, all can be in play simultaneously (Rundell & Price, 2009). Simple persistence in isolation can contribute to speciation, as can divergent selection across ecological or behavioural dimensions (Coyne & Orr, 1989; Sobel

et al., 2010). All this points to the need to dissect the speciation continuum (Shaw & Mullen, 2014) using diverse data types and at multiple scales if we are to reveal the myriad ways in which new species can form.

A final consideration is how to categorize lineages across the grey zone of speciation with regard to taxonomy and conservation (Coates et al., 2018). Ideally, ongoing gene flow in sympatry or across contact zones should be assessed to distinguish intraspecific from interspecific variation (Chambers et al., 2022; Unmack et al., 2022). Adequately sampling across contact zones can be difficult, however, and is not possible when populations are allopatric—as is the case for many lineages of *H. planiceps* that occur on disjunct rock formations. Considering this, and the possibility of introgression among distantly related lineages (i.e., plan-L and plan-H), we would caution a conservative approach were taxonomic decisions to be based solely on our results here, perhaps recognizing only the extremely deeply divergent plan-M lineage as a distinct species pending further study. Dense sampling across potential contact zones in combination with genome-wide sequence data could reveal the presence and extent of ongoing gene flow (presently underway), and thus whether these lineages are reproductively isolated species. Results from those lineages in contact—in combination with data on morphology and chemical signals—could then be used to infer whether allopatric lineages of varying levels of divergence are likely to be reproductively isolated (Singhal et al., 2018). While the taxonomic treatment of allopatric populations is difficult and always involves some degree of subjectivity, integrative taxonomic approaches such as these root such decisions in biology and better avoid taxonomic inflation (Padial et al., 2010; Unmack et al., 2022). These considerations, however, do not address how such lineages should be regarded with respect to conservation, which is much more subjective. Given that the 17 lineages of *H. planiceps* are each deeply divergent enough that their species status itself is in question, and that many are isolated to relatively small rocky areas, we suggest that each of the 17 lineages be treated as an evolutionary significant unit (ESU; Moritz, 1994), at least for the time being. As such, they have been included as taxa in analyses of regional phyloendemism and conservation priorities (Oliver et al., 2017; Rosauer et al., 2018).

## AUTHOR CONTRIBUTIONS

S.M.Z. and C.M. conceived the study with input on design and execution from all co-authors, acquired funding, and wrote the manuscript. Fieldwork was undertaken by S.M.Z., L.G.T., C.J.H. and C.M. Laboratory work for mtDNA sequencing was done by L.G.C. Phylogenetic analyses were performed by S.M.Z., L.C.T. and L.G.T; all other analyses were performed by S.M.Z. with input on phenotypic analyses from M.H. and C.J.H. All figures were created by S.M.Z. All authors contributed to editing the manuscript.

## ACKNOWLEDGEMENTS

We thank: Gayleen Bourke and Renae Pratt for assistance with data acquisition; Sally Potter, Emily Roycroft and Mitzy Pepper for advice and inspiration; owners and managers of lands on which we collected samples, including the Bunuba and Wunambal Gaambera Aboriginal Corporations, Cecelia Myers, and the Australian Wildlife Conservancy; Paul Doughty of the Western Australian Museum and Gavin Dally of the Museum and Art Galleries of the Northern Territory for access to tissues and specimens; and the Australian Research Council (FL110100104 and DP210102267) and Australian Geographic Society for funding. Open access publishing facilitated by Australian National University, as part of the Wiley - Australian National University agreement via the Council of Australian University Librarians.

## CONFLICT OF INTEREST

The authors declare that they have no conflicts of interest.

## DATA AVAILABILITY STATEMENT

All data associated with this study are available at the Dryad Digital Repository: https://doi.org/10.5061/dryad.8kprr4xs1. Chemical data were acquired from: Zozaya, Stephen, Teasdale, Luisa, Moritz, Craig, Higgie, Megan, & Hoskin, Conrad. (2022). Data from: Composition of a chemical signalling trait varies with phylogeny and precipitation across an Australian lizard radiation. Dryad, Dataset, https://doi.org/10.5061/dryad.4j0zpc8dx.

## ORCID

*Stephen M. Zozaya* https://orcid.org/0000-0003-3451-3552

## REFERENCES

Aitchison, J. (1986). *The statistical analysis of compositional data*. Chapman & Hall.

Alföldi, J., di Palma, F., Grabherr, M., Williams, C., Kong, L., Mauceli, E., Russell, P., Lowe, C. B., Glor, R. E., Jaffe, J. D., Ray, D. A., Boissinot, S., Shedlock, A. M., Botka, C., Castoe, T. A., Colbourne, J. K., Fujita, M. K., Moreno, R. G., ten Hallers, B., … Lindblad-Toh, K. (2011). The genome of the green anole lizard and a comparative analysis with birds and mammals. *Nature*, *477*(7366), 587–591.

Ashman, L. G., Bragg, J. G., Doughty, P., Hutchinson, M. N., Bank, S., Matzke, N. J., Oliver, P., & Moritz, C. (2018). Diversification across biomes in a continental lizard radiation. *Evolution*, *72*(8), 1553–1569.

Avise, J. C., Walker, D., & Johns, G. C. (1998). Speciation durations and Pleistocene effects on vertebrate phylogeography. *Proceedings of the Royal Society of London. Series B: Biological Sciences*, *265*(1407), 1707–1712.

Baeckens, S., Martín, J., García-Roa, R., Pafilis, P., Huyghe, K., & Van Damme, R. (2018). Environmental conditions shape the chemical signal design of lizards. *Functional Ecology*, *32*(2), 566–580.

Bi, K., Vanderpool, D., Singhal, S., Linderoth, T., Moritz, C., & Good, J. M. (2012). Transcriptome-based exon capture enables highly cost-effective comparative genomic data collection at moderate evolutionary scales. *BMC Genomics*, *13*(1), 1–14.

Blom, M. P. K., Horner, P., & Moritz, C. (2016). Convergence across a continent: Adaptive diversification in a recent radiation of Australian lizards. *Proceedings of the Royal Society B: Biological Sciences*, *283*, 20160181.

Blomberg, S. P., Garland, T., Jr., & Ives, A. R. (2003). Testing for phylogenetic signal in comparative data: Behavioral traits are more labile. *Evolution*, *57*, 717–745.

Bouckaert, R., Heled, J., Kühnert, D., Vaughan, T., Wu, C. H., Xie, D., Suchard, M. A., Rambaut, A., & Drummond, A. J. (2014). BEAST

2: A software platform for Bayesian evolutionary analysis. *PLoS Computational Biology*, *10*(4), e1003537.

Boughman, J. W. (2002). How sensory drive can promote speciation. *Trends in Ecology and Evolution*, *17*, 571–577.

Bragg, J. G., Potter, S., Bi, K., & Moritz, C. (2016). Exon capture phylogenomics: Efficacy across scales of divergence. *Molecular Ecology Resources*, *16*(5), 1059–1068.

Butlin, R. (1987). Speciation by reinforcement. *Trends in Ecology & Evolution*, *2*(1), 8–13.

Campos, S. M., Pruett, J. A., Soini, H. A., Zúñiga-Vega, J. J., Goldberg, J. K., Vital-García, C., Hews, D. K., Novotny, M. V., & Martins, E. P. (2020). Volatile fatty acid and aldehyde abundances evolve with behavior and habitat temperature in Sceloporus lizards. *Behavioral Ecology*, *31*(4), 978–991.

Chambers, E. A., & Hillis, D. M. (2020). The multispecies coalescent over-splits species in the case of geographically widespread taxa. *Systematic Biology*, *69*(1), 184–193.

Chambers, E. A., Marshall, T. L., & Hillis, D. M. (2022). The importance of contact zones for distinguishing interspecific from intraspecific geographic variation. *Systematic Biology*, *syac056*.

Chan, K. O., Hutter, C. R., Wood, P. L., Jr., Su, Y. C., & Brown, R. M. (2022). Gene flow increases phylogenetic structure and inflates cryptic species estimations: A case study on widespread Philippine puddle frogs (*Occidozyga laevis*). *Systematic Biology*, *71*(1), 40–57.

Chernomor, O., Von Haeseler, A., & Minh, B. Q. (2016). Terrace aware data structure for phylogenomic inference from supermatrices. *Systematic Biology*, *65*(6), 997–1008.

Coates, D. J., Byrne, M., & Moritz, C. (2018). Genetic diversity and conservation units: Dealing with the species-population continuum in the age of genomics. *Frontiers in Ecology and Evolution*, *6*, 165.

Coyne, J. A., & Orr, H. A. (1989). Patterns of speciation in drosophila. *Evolution*, *43*(2), 362–381.

Coyne, J. A., & Orr, H. A. (2004). *Speciation*. Sinauer Associates.

Criscuolo, A., & Gribaldo, S. (2010). BMGE (block mapping and gathering with entropy): A new software for selection of phylogenetic informative regions from multiple sequence alignments. *BMC Evolutionary Biology*, *10*(1), 1–21.

Endler, J. A. (1992). Signals, signal conditions, and the direction of evolution. *The American Naturalist*, *139*(suppl), S125–S153.

Etienne, R. S., & Rosindell, J. (2012). Prolonging the past counteracts the pull of the present: Protracted speciation can explain observed slowdowns in diversification. *Systematic Biology*, *61*(2), 204–213.

Felsenstein, J. (1985). Confidence limits on phylogenies: An approach using the bootstrap. *Evolution*, *39*(4), 783–791.

Fenker, J., Tedeschi, L. G., Melville, J., & Moritz, C. (2021). Predictors of phylogeographic structure among codistributed taxa across the complex Australian monsoonal tropics. *Molecular Ecology*, *30*(17), 4276–4291.

Flouri, T., Jiao, X., Rannala, B., & Yang, Z. (2020). A Bayesian implementation of the multispecies coalescent model with introgression for phylogenomic analysis. *Molecular Biology and Evolution*, *37*(4), 1211–1223.

Fujita, M. K., Boore, J. L., & Moritz, C. (2007). Multiple origins and rapid evolution of duplicated mitochondrial genes in parthenogenetic geckos (*Heteronotia binoei*; Squamata, Gekkonidae). *Molecular Biology and Evolution*, *24*(12), 2775–2786.

Fujita, M. K., McGuire, J. A., Donnellan, S. C., & Moritz, C. (2010). Diversification and persistence at the arid-monsoonal interface: Australia-wide biogeography of the Bynoe's gecko (*Heteronotia binoei*; Gekkonidae). *Evolution*, *64*, 2293–2314.

Gadagkar, S. R., Rosenberg, M. S., & Kumar, S. (2005). Inferring species phylogenies from multiple genes: Concatenated sequence tree versus consensus gene tree. *Journal of Experimental Zoology Part B: Molecular and Developmental Evolution*, *304*(1), 64–74.

Gray, J. E. (1845). *Catalogue of the specimens of lizards in the collection of the British museum*. British Museum.

Guindon, S., Dufayard, J. F., Lefort, V., Anisimova, M., Hordijk, W., & Gascuel, O. (2010). New algorithms and methods to estimate maximum-likelihood phylogenies: Assessing the performance of PhyML 3.0. *Systematic Biology*, *59*(3), 307–321.

Hahn, C., Bachmann, L., & Chevreux, B. (2013). Reconstructing mitochondrial genomes directly from genomic next-generation sequencing reads—A baiting and iterative mapping approach. *Nucleic Acids Research*, *41*(13), e129.

Higgie, M., Chenoweth, S., & Blows, M. W. (2000). Natural selection and the reinforcement of mate recognition. *Science*, *290*(5491), 519–521.

Hoang, D. T., Chernomor, O., Von Haeseler, A., Minh, B. Q., & Vinh, L. S. (2018). UFBoot2: Improving the ultrafast bootstrap approximation. *Molecular Biology and Evolution*, *35*(2), 518–522.

Hoskin, C. J., & Higgie, H. (2010). Speciation via species interactions: The divergence of mating traits within species. *Ecology Letters*, *13*, 409–420.

Hoskin, C. J., Higgie, M., McDonald, K. R., & Moritz, C. (2005). Reinforcement drives rapid allopatric speciation. *Nature*, *437*(7063), 1353–1356.

Hoskin, C. J., Tonione, M., Higgie, M., MacKenzie, J. B., Williams, S. E., VanDerWal, J., & Moritz, C. (2011). Persistence in peripheral refugia promotes phenotypic divergence and speciation in a rainforest frog. *The American Naturalist*, *178*(5), 561–578.

Howard, D. J. (1993). Reinforcement: Origin, dynamics, and fate of an evolutionary hypothesis. In R. G. Harrison (Ed.), *Hybrid zones and the evolutionary process* (pp. 46–69). Oxford University Press.

Irwin, D., & Schluter, D. (2022). Hybridization and the coexistence of species. *The American Naturalist*, *200*(3), E93–E109.

Ji, J., Jackson, D. J., Leache, A., & Yang, Z. (2021). Significant cross-species gene flow detected in the *Tamias quadrivittatus* group of north American chipmunks. *BioRxiv*. https://doi.org/10.1101/2021.12.07.471567

Jolliffe, I. T., Learmonth, J. A., Pierce, G. J., Santos, M. B., Trendafilov, N., Zuur, A. F., Ieno, E. N., & Smith, G. M. (2007). Principal component analysis applied to harbour porpoise fatty acid data. In A. E. Zuur, A. E. N. Ieno, & G. M. Smith (Eds.), *Analysing ecological data* (pp. 515–527). Springer.

Kabir, M. S., Venkatesan, R., & Thaker, M. (2020). Multiple sensory modalities in diurnal geckos is associated with the signaling environment and evolutionary constraints. *Integrative Organismal Biology*, *2*(1), obaa027.

Kalyaanamoorthy, S., Minh, B. Q., Wong, T. K., Von Haeseler, A., & Jermiin, L. S. (2017). ModelFinder: Fast model selection for accurate phylogenetic estimates. *Nature Methods*, *14*(6), 587–589.

Katoh, K., Misawa, K., Kuma, K. I., & Miyata, T. (2002). MAFFT: A novel method for rapid multiple sequence alignment based on fast Fourier transform. *Nucleic Acids Research*, *30*(14), 3059–3066.

Kirkpatrick, M., & Ravigné, V. (2002). Speciation by natural and sexual selection: Models and experiments. *The American Naturalist*, *159*(S3), S22–S35.

Koehler, F. (2010). Three new species and two new genera of land snails from the Bonaparte archipelago in the Kimberley, Western Australia (Pulmonata, Camaenidae). *Molluscan Research*, *30*(1), 1–16.

Kozak, K. H., & Wiens, J. (2006). Does niche conservatism promote speciation? A case study in north American salamanders. *Evolution*, *60*(12), 2604–2621.

Lande, R. (1981). Models of speciation by sexual selection on polygenic traits. *Proceedings of the National Academy of Sciences*, *78*, 3721–3725.

Laver, R. J., Doughty, P., & Oliver, P. (2018). Origins and patterns of endemic diversity in two specialized lizard lineages from the Australian monsoonal tropics (*Oedura* spp.). *Journal of Biogeography*, *45*, 142–153.

Laver, R. J., Nielsen, S. V., Rosauer, D. F., & Oliver, P. M. (2017). Trans-biome diversity in Australian grass-specialist lizards (Diplodactylidae: *Strophurus*). *Molecular Phylogenetics and Evolution*, *115*, 62–70.

Leaché, A. D., Zhu, T., Rannala, B., & Yang, Z. (2019). The spectre of too many species. *Systematic Biology*, *68*(1), 168–181.

Martín, J., & López, P. (2014). Pheromones and chemical communication in lizards. In J. L. Rheubert, D. S. Siegel, & S. E. Trauth (Eds.), *Reproductive biology and phylogeny of lizards and tuatara* (pp. 43–75). CRC.

McKenna, A., Hanna, M., Banks, E., Sivachenko, A., Cibulskis, K., Kernytsky, A., Garimella, K., Altshuler, D., Gabriel, S., Daly, M., & DePristo, M. (2010). The genome analysis toolkit: A MapReduce framework for analyzing next-generation DNA sequencing data. *Genome Research*, *20*(9), 1297–1303.

Meyer, M., & Kircher, M. (2010). Illumina sequencing library preparation for highly multiplexed target capture and sequencing. *Cold Spring Harbor Protocols*, *2010*(6), pdb-prot5448.

Minh, B. Q., Schmidt, H. A., Chernomor, O., Schrempf, D., Woodhams, M. D., Von Haeseler, A., & Lanfear, R. (2020). IQ-TREE 2: New models and efficient methods for phylogenetic inference in the genomic era. *Molecular Biology and Evolution*, *37*(5), 1530–1534.

Moritz, C. (1994). Defining 'evolutionarily significant units' for conservation. *Trends in Ecology & Evolution*, *9*, 373–375.

Moritz, C., Fujita, M. K., Rosauer, D., Agudo, R., Bourke, G., Doughty, P., Palmer, R., Pepper, M., Potter, S., Pratt, R., Scott, M., Tonione, M., & Donnellan, S. (2016). Multilocus phylogeography reveals nested endemism in a gecko across the monsoonal tropics of Australia. *Molecular Ecology*, *25*(6), 1354–1366.

Moritz, C. C., Pratt, R. C., Bank, S., Bourke, G., Bragg, J. G., Doughty, P., Keogh, J. S., Laver, R. J., Potter, S., Teasdale, L. C., Tedeschi, L. G., & Oliver, P. M. (2018). Cryptic lineage diversity, body size divergence, and sympatry in a species complex of Australian lizards (*Gehyra*). *Evolution*, *72*(1), 54–66.

Nei, M. (1973). The theory and estimation of genetic distance. In N. E. Morton (Ed.), *Genetic structure of populations*. University Press of Hawaii.

Nei, M., & Li, W. H. (1979). Mathematical model for studying genetic variation in terms of restriction endonucleases. *Proceedings of the National Academy of Sciences*, *76*, 5269–5273.

Noor, M. A. (1999). Reinforcement and other consequences of sympatry. *Heredity*, *83*(5), 503–508.

Nosil, P., & Flaxman, S. M. (2011). Conditions for mutation-order speciation. *Proceedings of the Royal Society B: Biological Sciences*, *278*(1704), 399-407.

Ogilvie, H. A., Bouckaert, R. R., & Drummond, A. J. (2017). StarBEAST2 brings faster species tree inference and accurate estimates of substitution rates. *Molecular Biology and Evolution*, *34*, 2101–2114.

Oksanen, J., Blanchet, F. G., Friendly, M., Kindt, R., Legendre, P., McGlinn, D., Minchin, P. R., O'Hara, R. B., Simpson, G. L., & Solymos, P. (2017). *Vegan: Community ecology package*. R package version 2.4–2. https://cran.r-project.org/package.pvegan

Oliver, P. M., Ashman, L. G., Bank, S., Laver, R. J., Pratt, R. C., Tedeschi, L. G., & Moritz, C. C. (2019). On and off the rocks: Persistence and ecological diversification in a tropical Australian lizard radiation. *BMC Evolutionary Biology*, *19*(1), 1–15.

Oliver, P. M., Doughty, P., & Palmer, R. (2012). Hidden biodiversity in rare northern Australian vertebrates: The case of the clawless geckos (*Crenadactylus*, Diplodactylidae) of the Kimberley. *Wildlife Research*, *39*(5), 429–435.

Oliver, P. M., Laver, R. J., Martins, F. D. M., Pratt, R. C., Hunjan, S., & Moritz, C. (2017). A novel hotspot of vertebrate endemism and an evolutionary refugium in tropical Australia. *Diversity and Distributions*, *23*, 53–66.

Padial, J. M., Miralles, A., De la Riva, I., & Vences, M. (2010). The integrative future of taxonomy. *Frontiers in Zoology*, *7*(1), 1–14.

Pepper, M., Doughty, P., Fujita, M. K., Moritz, C., & Keogh, J. S. (2013). Speciation on the rocks: Integrated systematics of the *Heteronotia spelea* species complex (Gekkota; Reptilia) from Western and Central Australia. *PLoS One*, *8*, e78110.

Pepper, M., Fujita, M. K., Moritz, C., & Keogh, J. S. (2011). Palaeoclimate change drove diversification among isolated mountain refugia in the Australian arid zone. *Molecular Ecology*, *20*(7), 1529–1545.

Pepper, M., & Keogh, J. S. (2014). Biogeography of the Kimberley, Western Australia: A review of landscape evolution and biotic response in an ancient refugium. *Journal of Biogeography*, *41*(8), 1443–1455.

Pfeifer, B., Wittelsbürger, U., Ramos-Onsins, S. E., & Lercher, M. J. (2014). PopGenome: An efficient swiss army knife for population genomic analyses in R. *Molecular Biology and Evolution*, *31*(7), 1929–1936.

Potter, S., Eldridge, M. D. B., Taggart, D. A., & Cooper, S. J. B. (2012). Multiple biogeographical barriers identified across the monsoon tropics of northern Australia: Phylogeographic analysis of the *brachyotis* group of rock-wallabies. *Molecular Ecology*, *21*, 2254–2269.

Potter, S., Xue, A. T., Bragg, J. G., Rosauer, D. F., Roycroft, E. J., & Moritz, C. (2018). Pleistocene climatic changes drive diversification across a tropical savanna. *Molecular Ecology*, *27*(2), 520–532.

R Core Team. (2020). *R: A language and environment for statistical computing (version 4.0. 3)[computer software]*. R Foundation for Statistical Computing.

Rambaut, A., Drummond, A. J., Xie, D., Baele, G., & Suchard, M. A. (2018). Posterior summarisation in Bayesian phylogenetics using tracer 1.7. *Systematic Biology*, *67*, 901–904.

Ranwez, V., Harispe, S., Delsuc, F., & Douzery, E. J. P. (2011). MACSE: Multiple alignment of coding sequences accounting for frameshifts and stop codons. *PLoS One*, *6*, e22594.

Riedel, J., Zozaya, S. M., Hoskin, C. J., & Schwarzkopf, L. (2021). Parallel evolution of toepads in rock-dwelling lineages of a terrestrial gecko (Gekkota: Gekkonidae: *Heteronotia binoei*). *Zoological Journal of the Linnean Society*, *193*, 636–654.

Ritchie, M. G. (2007). Sexual selection and speciation. *Annual Review of Ecology, Evolution, and Systematics*, *38*, 79–102.

Rosauer, D. F., Byrne, M., Blom, M. P., Coates, D. J., Donnellan, S., Doughty, P., Keogh, J. S., Kinloch, J., Laver, R. J., Myers, C., & Oliver, P. M. (2018). Real-world conservation planning for evolutionary diversity in the Kimberley, Australia, sidesteps uncertain taxonomy. *Conservation Letters*, *11*(4), e12438.

Rosenblum, E. B., Sarver, B. A., Brown, J. W., Des Roches, S., Hardwick, K. M., Hether, T. D., Eastman, J. M., Pennell, M. W., & Harmon, L. J. (2012). Goldilocks meets Santa Rosalia: An ephemeral speciation model explains patterns of diversification across time scales. *Evolutionary Biology*, *39*(2), 255–261.

Roux, C., Fraisse, C., Romiguier, J., Anciaux, Y., Galtier, N., & Bierne, N. (2016). Shedding light on the grey zone of speciation along a continuum of genomic divergence. *PLoS Biology*, *14*(12), e2000234.

Roycroft, E. J., Moussalli, A., & Rowe, K. C. (2020). Phylogenomics uncovers confidence and conflict in the rapid radiation of Australo-Papuan rodents. *Systematic Biology*, *69*(3), 431–444.

Rundell, R. J., & Price, T. D. (2009). Adaptive radiation, nonadaptive radiation, ecological speciation and nonecological speciation. *Trends in Ecology & Evolution*, *24*(7), 394–399.

Schluter, D. (2009). Evidence for ecological speciation and its alternative. *Science*, *323*, 737–741.

Seehausen, O., Terai, Y., Magalhaes, I. S., Carleton, K. L., Mrosso, H. D. J., Miyagi, R., van der Sluijs, I., Schneider, M. V., Maan, M. E., Tachida, H., Imai, H., & Okada, N. (2008). Speciation through sensory drive in cichlid fish. *Nature*, *455*, 620–626.

Seo, T. K., Kishino, H., & Thorne, J. L. (2005). Incorporating gene-specific variation when inferring and evaluating optimal evolutionary tree topologies from multilocus sequence data. *Proceedings of the National Academy of Sciences*, *102*(12), 4436–4441.

Shaw, K. L., & Mullen, S. P. (2014). Speciation continuum. *Journal of Heredity*, *105*(S1), 741–742.
Singhal, S., Hoskin, C. J., Couper, P., Potter, S., & Moritz, C. (2018). A framework for resolving cryptic species: A case study from the lizards of the Australian wet tropics. *Systematic Biology*, *67*(6), 1061–1075.
Singhal, S., & Moritz, C. (2013). Reproductive isolation between phylogeographic lineages scales with divergence. *Proceedings of the Royal Society B: Biological Sciences*, *280*(1772), 20132246.
Smadja, C., & Butlin, R. K. (2009). On the scent of speciation: The chemosensory system and its role in premating isolation. *Heredity*, *102*, 77–97.
Sobel, J. M., Chen, G. F., Watt, L. R., & Schemske, D. W. (2010). The biology of speciation. *Evolution: International Journal of organic evolution*, *64*(2), 295–315.
Storr, G. M. (1989). A new *Heteronotia* (Lacertilia: Gekkonidae) from Western Australia. *Records of the Western Australian Museum*, *14*, 269–273.
Sukumaran, J., & Knowles, L. L. (2017). Multispecies coalescent delimits structure, not species. *Proceedings of the National Academy of Sciences*, *114*(7), 1607–1612.
Unmack, P. J., Adams, M., Hammer, M. P., Johnson, J. B., Gruber, B., Gilles, A., Young, M., & Georges, A. (2022). Plotting for change: An analytical framework to aid decisions on which lineages are candidate species in phylogenomic species discovery. *Biological Journal of the Linnean Society*, *135*, 117–137.
Warton, D. I., & Hui, F. K. (2011). The arcsine is asinine: The analysis of proportions in ecology. *Ecology*, *92*, 3–10.
Wiens, J. J. (2004). Speciation and ecology revisited: Phylogenetic niche conservatism and the origin of species. *Evolution*, *58*(1), 193–197.
Zhang, C., Rabiee, M., Sayyari, E., & Mirarab, S. (2018). ASTRAL-III: Polynomial time species tree reconstruction from partially resolved gene trees. *BMC Bioinformatics*, *19*(6), 15–30.
Zozaya, S. M., Higgie, M., Moritz, C., & Hoskin, C. J. (2019). Are pheromones key to unlocking cryptic lizard diversity? *American Naturalist*, *194*, 168–182.
Zozaya, S. M., Teasdale, L. C., Moritz, C., Higgie, M., & Hoskin, C. J. (2022a). Composition of a chemical signalling trait varies with phylogeny and precipitation across an Australian lizard radiation. *Journal of Evolutionary Biology*, *35*, 919–933.
Zozaya, S. M., Teasdale, L. C., Moritz, C., Higgie, M., & Hoskin, C. J. (2022b). *Composition of a chemical signalling trait varies with phylogeny and precipitation across an Australian lizard radiation*. Dryad, Dataset. 10.5061/dryad.4j0zpc8dx

## SUPPORTING INFORMATION

Additional supporting information can be found online in the Supporting Information section at the end of this article.

**How to cite this article:** Zozaya, S. M., Teasdale, L. C., Tedeschi, L. G., Higgie, M., Hoskin, C. J., & Moritz, C. (2023). Initiation of speciation across multiple dimensions in a rock-restricted, tropical lizard. *Molecular Ecology*, *32*, 680–695. https://doi.org/10.1111/mec.16787